ELASTIC STRESSES IN A FLEXIBLY RESTRAINED SOIL MASS OR OTHER

By Farid A. Chouery, PE, SE[1], and John F. Stanton, PE, Ph. D.[2]

Abstract: The paper addresses the problem of soil pressure exerted on timber lagging or other supporting an open cut. Using an elastic approach, the analysis determines the pressure behind lagging, demonstrates the existence of arching, and investigates the influence of different parameters on the extent of arching. Exact solutions, first for one bay of lagging and then for infinite number of bays of lagging are presented. Numerical examples are provided.

Introduction:

To design a retaining wall satisfactorily, the pressure exerted by the soil mass on the wall must be known. If the wall cross section is constant along the length of the wall, the pressure is assumed to vary only with depth and to be independent of position along the length of the wall. The classical methods for finding the distribution of horizontal pressure, such as Rankine and Coulomb methods, are based on the assumption that friction is fully mobilized.

Temporary shoring walls are frequently made from soldier piles with timber lagging spanning between them; see Fig. 1. In this the soil pressure varies along the wall, because of the flexibility of the lagging.

---

[1]Structural, Electrical and Foundation Engineer, FAC Systems Inc. Seattle, WA

[2]Professor of Civil Engineering, University of Washington, Seattle, WA 98195

Collapse of the soil is prevented partly by the resistance of the lagging, and partly by the soil itself arching between the soldier piles. Both site observations [6] and White's discussion [7] lead to this conclusion.

This redistribution of pressure, known as arching [4], is related to the way shoring is usually constructed. The lagging beams are placed on the back face of the front flange of soldier piles. A slight overcut is made behind the flange to facilitate placement of the boards. They are inserted diagonally and then rotated to their final horizontal orientation. Alternatively, the lagging can be installed in front of the pile after welding a threaded stud to the pile. A nut and plate are placed to hold the lagging to the pile. In both cases, the intervening space behind the boards is filled with soil. The soil should completely fill the void, but should not be packed so tight as to induce flexure. Similar loading occurs when backfill is placed against a retaining wall and is compacted layer by layer. This may develop high lateral earth pressures as explained by Brown [1]. A third way of placing lagging occurs in shafts. The lagging is installed vertically in the shaft, then a circular steel ring is put together at the bottom of the shaft, raised up to the proper position and then shims are put in to ensure contact between soil, lagging and ring.

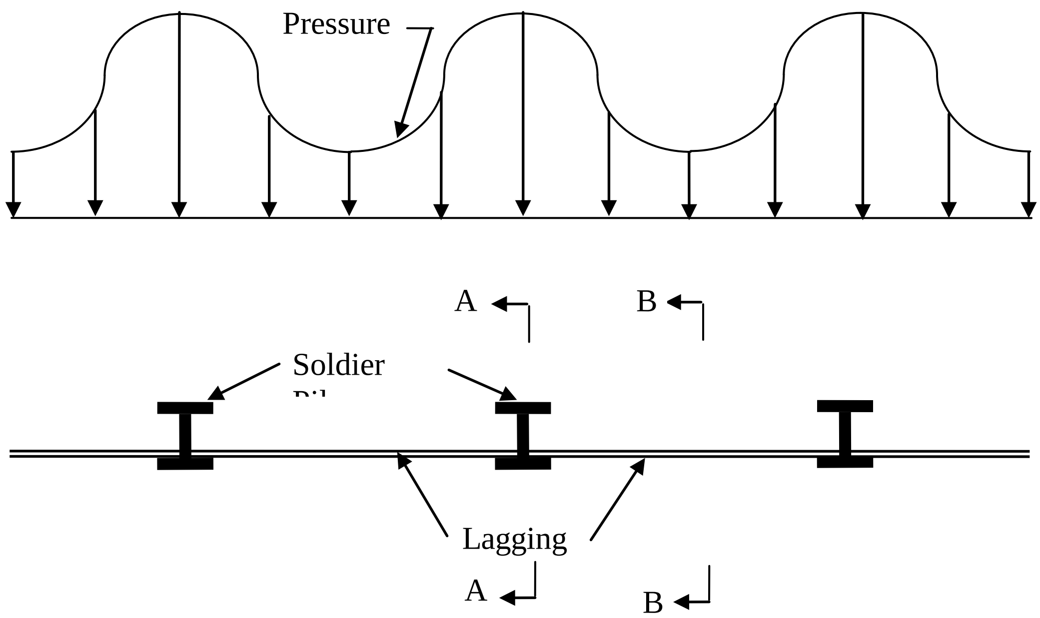

PLAN

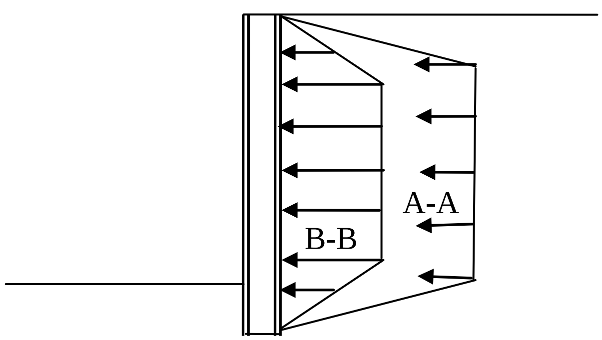

SECTION

FIG. 1 Approximate distribution of soil pressure.

If the soil behaves like an equivalent fluid, the vertical distribution of pressure on the lagging does not change as the cut deepens and the pressure on the lagging is zero when it is installed. However time dependent movements of the soil may occur. Any changes in the vertical distribution of pressure, due to the time dependent movement of soil or due to deepening of the cut will cause pressures on the lagging. This in turn gives rise to a redistribution of load, resulting in decrease of pressure at mid span of the lagging and a corresponding increase at the soldier piles. The vertical distribution of horizontal pressure on the lagging and soldier piles is about the same as on a wall with constant cross section namely, trapezoidal, (Fig.1) triangular, rectangular, etc.

Lagging is presently designed empirically. The simplest ways to account for its flexibility are to reduce the design earth pressure or to increase the allowable lagging stresses by some arbitrary factor. The former is more common [2,5], and a 50% reduction is common. The New York city transit authority takes the latter approach, and increases the allowable flexure stress in the lagging by 50%. This method is more costly than taking 50% reduction on the earth pressure.

The objective of this paper is to perform a rational analysis of pressure behind lagging, to demonstrate the existence of arching, and to investigate the influence of different parameters on the extent of arching. Classical small deflection elasticity is used for the analysis. Although soils behave as linear elastic materials only at small strains, the rationale for the use of elastic theory is the tractability of the solution. A linear constitutive relation is usually chosen because of the lack of defensible alternatives.

The response of the lagging is calculated here first for a single bay of lagging between two soldier piles, then for multiple bays. In each case both the exact solution and a simpler approximate one based on collocation functions are developed.

Exact Solution-One Bay Lagging:

The problem is to find the bending moments in the lagging and the pressure exerted by the soil. This amounts to satisfying equilibrium and compatibility in the soil mass, together with the boundary conditions. A plan view of a retaining wall, consisting of a single bay of lagging restraining a soil mass, is shown in Fig. 2. Let the displacement of the soil on the lagging at $y = 0$ be $v_0(z)$ for $-b < z < b$. The back of the wall is assumed to be frictionless.

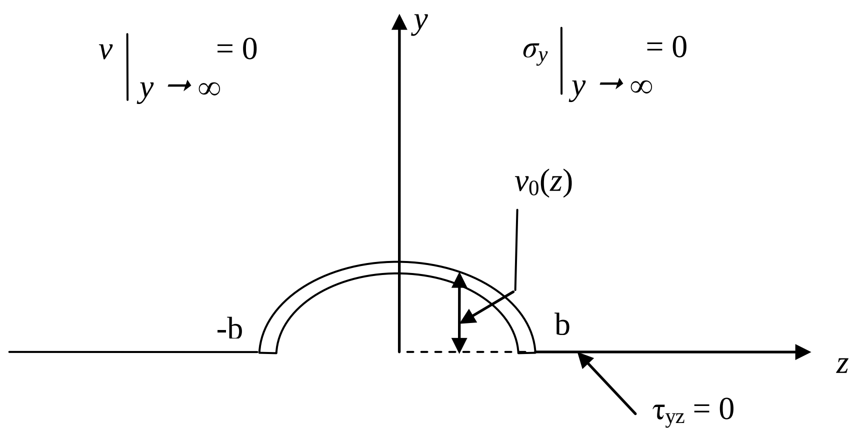

FIG. 2 Plan View of a Wall Consisting of a Single Bay of Lagging: Soil Displacement and Boundary Conditions.

Equilibrium and compatibility within the soil mass can be satisfied by the stress function [3]

$$\Phi = \int_0^\infty \frac{D(\alpha)}{\alpha^2}(1+\alpha y)e^{-\alpha y}\cos\alpha z \, d\alpha \quad \text{...} \quad (1)$$

Where $D(\alpha)$ is an arbitrary constant to be found later. Φ satisfies the bi-harmonic equation:

$$\frac{\partial^4\Phi}{\partial z^4}+\frac{2\partial^4\Phi}{\partial z^2\partial y^2}+\frac{\partial^4\Phi}{\partial y^4}=0 \quad \text{(2)}$$

Therefore

$$\sigma_y=\frac{\partial^2\Phi}{\partial z^2}=-\int_0^\infty D(\alpha)(1+\alpha y)e^{-\alpha y}\cos\alpha z\, d\alpha \quad \text{(3)}$$

$$\sigma_z=\frac{\partial^2\Phi}{\partial y^2}=-\int_0^\infty D(\alpha)(1-\alpha y)e^{-\alpha y}\cos\alpha z\, d\alpha \quad \text{(4)}$$

$$\tau_{zy}=-\frac{\partial^2\Phi}{\partial z\partial y}=-\int_0^\infty D(\alpha)\,\alpha y\, e^{-\alpha y}\sin\alpha z\, d\alpha \quad \text{(5)}$$

$$\varepsilon_y=\frac{\partial v}{\partial y}=\beta\sigma_y-\rho\sigma_z \quad \text{(6)}$$

where $ß = (1 - \mu^2)/E_s$, $\rho = \mu(1 + \mu)/E_s$, μ is Poisson's ratio and E_s is the soil modulus. σ_y, σ_z are the direct stresses and τ_{zy} is the shear stress. ε_y is the strain in the y direction. These values for $ß$ and ρ are appropriate for a horizontal slice of soil which exhibits plane strain behavior. For plane stress, $ß = 1/E_s$ and $\rho = \mu/E_s$. The true three dimensional state of stress lies somewhere between these two, and the two dimensional representation used here is thus an approximation. Values of $ß$ and ρ appropriate for some intermediate condition could easily be used.

Solving for the displacement $v(z)$ at $y = 0$ in the y direction, yields

$$v\Big|_{y=0} = \int_0^{\infty} \frac{2\beta D}{\alpha} \cos \alpha z \, d\alpha = v_0(z) \quad \text{...(7)}$$

The value of $D(\alpha)$ can be found by imposing the boundary conditions at the back of the wall. The displacement there, $v_0(z)$, is symmetrical about $z = 0$ and is represented by its Fourier transform as

$$v_0 = (2/\pi)\int_0^{\infty} \cos \alpha z \, d\alpha \int_0^b v_0(\lambda) \cos \lambda\alpha \, d\lambda \quad \text{..(8)}$$

Comparing this with Eq. 7 yields

$$D = \frac{\alpha}{\pi\beta}\int_0^b v_0(\lambda) \cos \lambda\alpha \, d\lambda$$

Substituting this value in Eq. 3, integrating the Laplace transform then setting $y = 0$ and adding the uniform pressure p, yields

$$\sigma\Big|_{y=0} = \frac{1}{2\pi\beta}\int_0^b v_0(\lambda)\left[\frac{1}{(z+\lambda)^2} + \frac{1}{(z-\lambda)^2}\right] d\lambda - p \quad \text{..(10)}$$

Where p is the horizontal pressure of the soil, and is positive.

This pressure acts as a load on a piece of lagging s wide (in the x direction) so

$$\frac{EI}{s}\frac{d^4 v_0(z)}{dz^4} = \sigma\Big|_{y=0} = \frac{1}{2\pi\beta}\int_0^b v_0(\lambda)\left[\frac{1}{(z+\lambda)^2}+\frac{1}{(z-\lambda)^2}\right]d\lambda - p \text{ ……………………(11)}$$

Where E is the modulus of elasticity of the lagging and I is its moment of inertia. This integral equation in v_0 cannot be solved directly so a series solution is obtained using

$$v_0(z) = -\delta\sum_{i=0}^{\infty}\alpha_i\left[\frac{z}{b}\right]^{2i} \text{ …………………………………………………………....……….(12)}$$

where δ=(5pb^4s)/(24EI) which is the central deflection of a beam of length 2b due to a uniform load, and α_i are constants to be determined. Integrating Eq. 11 and replacing the natural log terms by their Taylor series expansions eventually gives

$$v_0(z) = -\frac{s\delta b^3}{\pi\beta EI}\sum_{k=1}^{\infty}\frac{\eta^{2k+2}}{2k(2k+1)(2k+2)}\sum_{j=0}^{\infty}\frac{\alpha_j}{2j-2k-1} - \frac{spb^4\eta^4}{24EI} + \frac{s\overline{C}_0 b^2\eta^2}{2EI} + \overline{C}_1 \text{ …………..(13)}$$

Where $\eta = z/b$, C_0 and C_1 are constants of integration. Now combining Eq. 12 and Eq. 13 gives

$$B\sum_{i=0}^{\infty}\alpha_i\eta^{2i} = \sum_{k=1}^{\infty}\frac{\eta^{2k+2}}{2k(2k+1)(2k+2)}\sum_{j=0}^{\infty}\frac{\alpha_j}{2j-2k+1} + \frac{B\eta^4}{5} + \frac{BC_0\eta^2}{2} + BC_1 \text{ ………………….(14)}$$

Where $C_0 = -sb^2\overline{C}_0/(\delta EI)$, $C_1 = -\overline{C}_1/\delta$, $A=sb^3/(2\beta EI)$ and $B=\pi/(2A)$.

By equating the coefficient of η^{2i} on each side of Eq. 14, the following infinite system of linear equations is obtained:

$$\begin{vmatrix} 1 & 0 & 0 & 0 & \rightarrow & 0 \\ 0 & 1 & 0 & 0 & \rightarrow & 0 \\ -1 & 1 & 1/3\text{-}4\cdot 3\cdot 2\cdot B & 1/5 & \rightarrow & 0 \\ -1/3 & -1 & 1 & 1/3\text{-}6\cdot 5\cdot 4\cdot B & \rightarrow & 0 \\ \downarrow & \downarrow & \downarrow & \downarrow & \downarrow & \downarrow \\ 0 & 0 & 0 & 0 & 0 & 1 \end{vmatrix} \begin{vmatrix} \alpha_0 \\ \alpha_1 \\ \alpha_2 \\ \alpha_3 \\ \downarrow \\ \alpha_\infty \end{vmatrix} = C_1 \begin{vmatrix} 1 \\ 0 \\ 0 \\ 0 \\ \downarrow \\ 0 \end{vmatrix} + C_0/2 \begin{vmatrix} 0 \\ 1 \\ 0 \\ 0 \\ \downarrow \\ 0 \end{vmatrix} -24B/5 \begin{vmatrix} 0 \\ 0 \\ 1 \\ 0 \\ \downarrow \\ 0 \end{vmatrix} \quad \text{............ (15)}$$

The true solution to this set of equations is obtained by taking an infinite number of α_i and the corresponding square matrix. Tests with a finite number of α_i showed that the α_i diminish rapidly with increasing i, regardless of the number of equations used.

Secondly, ignoring the α_i corresponding to high i values has very little influence on the numerical value obtained for the first, more important terms in the α_i series. 30 terms were found to give at least 4-digit accuracy. For A=16.5 (the most sensitive condition), C_0 and C_1 for a simply supported beam were found to be -0.4812 and 0.2297, leading to $R_m = M_{\max}/(pb^2/2) = 0.20053$, and $R_v = V_{\max}/(-pb) = 0.50494$, and $\sigma_y(0) \approx 0$. Fig. 3 shows the modification factors R_m and R_v of maximum shear and moment divided by the maximum shear and moment of a uniformly loaded simple beam of length 2*b* and pressure *p*, versus *A*.

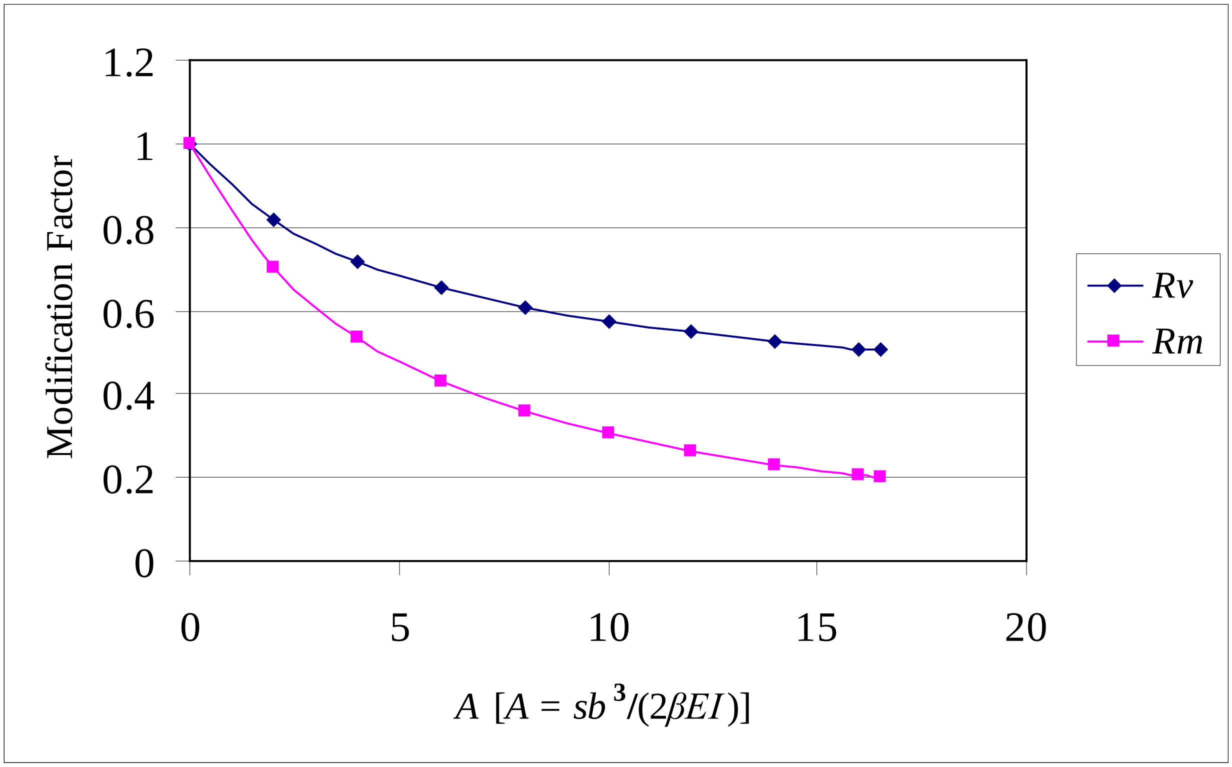

FIG. 3 Dimensionless Plot of Modification factors (R_v and R_m) – One Bay Lagging

Approximate Solution using collocation Functions:

The exact solution outlined above suffers from the disadvantage that, in the matrix equation for α_i, the coefficients in the series for $v_0(z)$ the deflected shape of the lagging, are difficult to find. An alternative is to start with an approximate, kinematically admissible solution, and then to develop successive improvements to it. This may be done by substituting the approximate $\bar{v}_0$ for $v_0(\lambda)$ in Eq. 11, and integrating four times to obtain a better $\tilde{v}_0(z)$. Starting with a parabola

$$\bar{v}_0(z) = -d_0\ \delta\,[1-(\eta)^2] \qquad (16)$$

Where $\eta = z/b$ and d_0 is a dimensionless constant to be determined. Substituting in Eq. 11 and integrating with respect to z yields the shear

$$-V(\eta) = \frac{EI}{s} v_0'''(\eta) = \frac{\delta d_0}{\pi\beta} w_0'''(\eta) - pb\eta \qquad (17)$$

Where $w_0'''(\eta) = \left[\eta + \frac{1-\eta^2}{2}\ln\left|\frac{1+\eta}{1-\eta}\right|\right]$

When integrating Eq. 17 to obtain the deflection, two non-zero constants of integration will be obtained, C_2 and C_3. These constants can be determined from the boundary conditions of a simple span beam, thus

$$C_2 = -\frac{2\ln 2+1}{3}\frac{\delta d_0 b}{\pi\beta} + p\frac{b^2}{2} \quad (18)$$

$$C_3 = -\frac{2\ln 2-1}{5}\frac{\delta d_0 b^3 s}{\pi\beta EI} - \frac{sb^2}{2EI}C_2 + \frac{spb^4}{24EI} \quad (19)$$

The improved approximation for the deflection then becomes

$$\tilde{v}_0(\eta) = d_0\,\delta\left[Aw_0(\eta) + \bar{d}_0(-\eta^4/5 + 6\eta/5 + 1)\right] \quad (20)$$

Where $A=sb^3/(2ßEI)$, $\bar{d}_0 = 1/d_0$. Note that w_0 and w_0'' are zero at η =1. If the solution was exact, $\bar{v}_0(z)$ and $\tilde{v}_0(z)$ would be identical. Since it is approximate, the error between $\bar{v}_0(z)$ and $\tilde{v}_0(z)$ can be minimized in a least squares sense to give

$$d_0 = 1/(0.2030123A + 255/248) \quad (21)$$

By replacing δ by $5pb^4s/(24EI)$ in Eq. 16, the end shear at η =1 divided by $-pb$ is obtained

$$R_v = \frac{V_{max}}{-pb} = -\frac{0.1326A}{0.2030123A + 255/248} + 1 \quad (22)$$

Similarly the midspan moment at η = 0 divided by $pb^2/2$ can be found using C_2 of Eq. 18

$$R_m = \frac{M_{\max}}{0.5pb^2} = -\frac{0.211A}{0.2030123A + 255/248} + 1 \quad (23)$$

These are compared in Table 1 with the exact values of the modification factors R_m and R_v. The maximum error is 0.8%, suggesting that the approximate results are quite accurate enough for practical purposes.

Table 1

Comparison of modification factors on Shear and Moment				
A	R_v Exact	R_v Approx	R_m Exact	R_m Approx
0	1	1	1	1
2	0.81976	0.81509	0.70068	0.70577
4	0.71865	0.71178	0.53476	0.54137
6	0.65356	0.64582	0.42949	0.43640
8	0.60790	0.60005	0.35686	0.36357
10	0.57392	0.56643	0.30381	0.31008
12	0.54752	0.54069	0.26343	0.26913
14	0.52632	0.52036	0.23171	0.23676
16	0.50885	0.50388	0.20616	0.21055
16.5	0.50494	0.50024	0.20053	0.20475

Differentiation of Eq. 17 gives the pressure on the back of the lagging

$$\sigma_y(\eta)/p = \frac{5}{12\pi}\left[\frac{A}{0.2030123A + 255/248}\right]\left[2 - \eta \ln\left|\frac{\eta+1}{\eta-1}\right|\right] - 1 \ldots\ldots\ldots\ldots\ldots\ldots\ldots\ldots\ldots\ldots(24)$$

and is shown as a function of η in Fig. 4 for various A values. A is a measure of the relative stiffness of the soil and lagging. It is zero when the lagging is very stiff, in which case the soil pressure along it is uniform. When A reaches 16.5, the soil is stiff enough to generate extensive arching action, and the soil pressure at midspan of the lagging drops to zero. The solutions for values of A larger than 16.5 are not valid because they imply tension between soil and lagging. This is unlikely in practice.

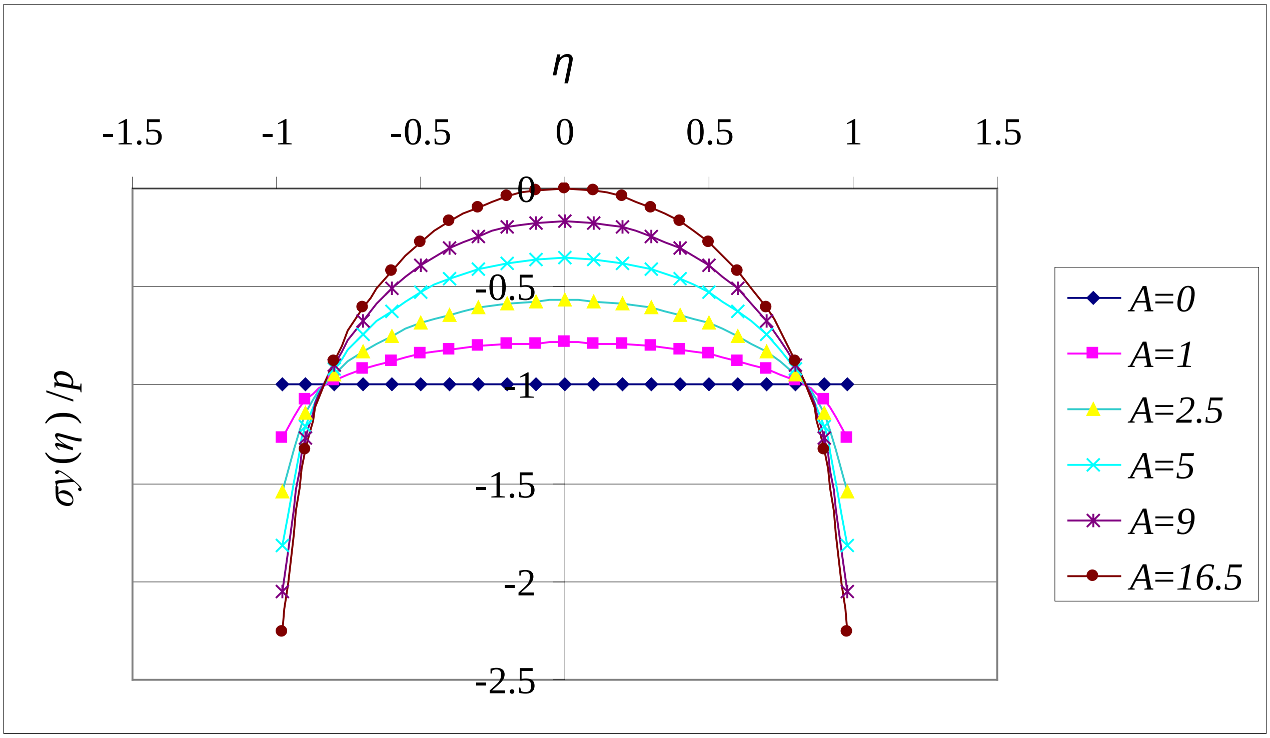

FIG. 4 Plot of Pressure Versus η – One Bay Lagging

Infinite Number of Bays of Lagging:

In practice, lagging is likely to exist over a number of adjacent bays, instead of just one bay. The pressure behind it and the moments and shears in it can be found using techniques similar to those outlined above. The displaced shape along the lagging bays is now periodic and symmetric about the *y* axis (see Fig. 5), so a Fourier cosine series instead of a Fourier integral is used. Therefore

$$v_0(z) = \sum_{n=\varphi}^{\infty} a_n \cos \alpha_n z \qquad (25)$$

Where $\alpha_n = n\pi/(b+t)$, and φ is a symbol indicating at the $n = 0$ term the coefficient a_0 is replaced by $a_0/2$. The stress function

$$\Phi = \sum_{n=\varphi}^{\infty} \frac{D_n}{\alpha_n^{\ 2}} (1+\alpha_n y)\, e^{-\alpha_n y} \cos \alpha_n z \quad \text{.......} (26)$$

satisfies the bi-harmonic equation and the boundary conditions. Stresses are given by

$$\sigma_y = -\sum_{n=\varphi}^{\infty} D_n \,(1+\alpha_n y)\, e^{-\alpha_n y} \cos \alpha_n z \quad \text{.......} (27)$$

$$\sigma_z = -\sum_{n=\varphi}^{\infty} D_n \,(1-\alpha_n y)\, e^{-\alpha_n y} \cos \alpha_n z \quad \text{.......} (28)$$

so that

$$v_0(z) = -\int_0^{\infty} \varepsilon_y \, dy = \sum_{n=\varphi}^{\infty} \frac{D_n}{\alpha_n} 2\beta \cos \alpha_n z \quad \text{.......} (29)$$

Combining Eq. 25 with 29 shows that

$D_n = \alpha_n a_n/(2ß)$ .... (30)

from which, when the uniform pressure is added,

$$\sigma_y\Big|_{y=0} = -\sum_{n=\varphi}^{\infty} \frac{\alpha_n a_n}{2\beta} \cos \alpha_n z - p \qquad (31)$$

Since

$$\int_0^{b+t} \sigma_y dz = -p(b+t) \qquad (32)$$

the first term in the series of Eq. 31 must be zero, so the lower summation limit can be changed to 1.

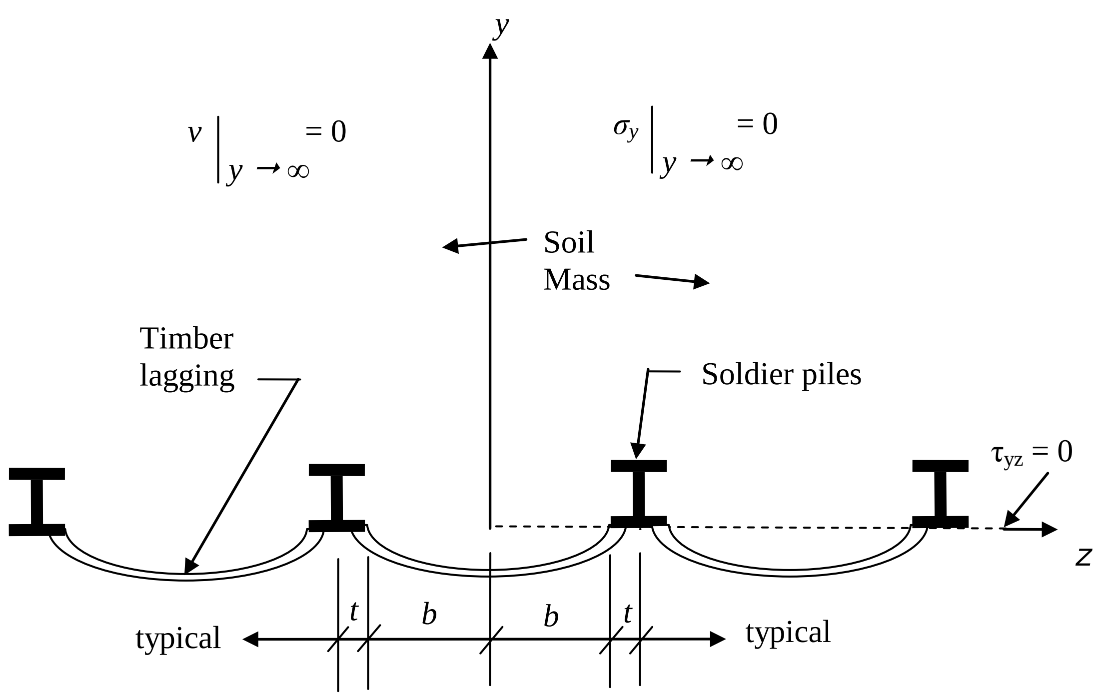

FIG. 5. Plan View of Displacement of Soil Mass for a Wall

Consisting of Soldier Piles and Lagging.

From the Fourier series definition a_n can be written as

$$a_n = \frac{2}{t+b}\int_0^b v_0(\lambda)\cos\alpha_n\lambda \; d\lambda \text{ .... (33)}$$

Substituting Eq. 33 in 31 and integrating twice with respect to z to find the moment, yields

$$\frac{EI}{s}v_0''(z) = \frac{1}{(t+b)\beta}\sum_{n=1}^{\infty}\int_0^b v_0(\lambda)\frac{\cos\alpha_n\lambda\cos\alpha_n z}{\alpha_n}\,d\lambda - \frac{pz^2}{2} + C_4$$

…................... (34)

$$= \frac{1}{2\pi\beta}\int_0^b v_0(\lambda)\left\{\sum_{n=1}^{\infty}\frac{\cos\left[\frac{\pi n(\lambda+z)}{t+b}\right]}{n} + \frac{\cos\left[\frac{\pi n(\lambda-z)}{t+b}\right]}{n}\right\}d\lambda - \frac{pz^2}{2} + C_4$$

Where C_4 is a constant of integration. Since $\pi(\lambda \pm z)/(t+b)$ is less than 2π for all λ and z the identity

$$\sum_{k=1}^{\infty}\frac{\cos kz}{k} = -\ln\left[2\sin\left(\frac{z}{2}\right)\right] \text{ .... (35)}$$

can be used. Thus Eq. 34 can be written as

$$\frac{EI}{s}v_0''(z) = -\frac{1}{2\pi\beta}\int_{-b}^{b} v_0(\lambda)\ln\left[2\sin\frac{\pi(\lambda+z)}{2(t+b)}\right]d\lambda - \frac{pz^2}{2} + C_4 \text{ ………..………………… (36)}$$

and the shear is

$$\frac{EI}{s} v_0'''(z) = -\frac{1}{4\beta(t+b)} \int_{-b}^{b} v_0(\lambda) \cot\left[\frac{\pi(\lambda+z)}{2(t+b)}\right] d\lambda - pz \quad (37)$$

and by using integration by parts the stress is

$$\frac{EI}{s} v_0^{(4)}(z) = \frac{1}{4\beta(t+b)} \int_{-b}^{b} v_0'(\lambda) \cot\left[\frac{\pi(\lambda+z)}{2(t+b)}\right] d\lambda - p \quad (38)$$

Eq. 38 is a statement of equilibrium of forces normal to the lagging, expressed in terms of the unknown displacement field $v_0(z)$. In parallel with the solution for a single bay, it is possible either to assume an approximate function (eg a parabola) for $v_0(z)$ and then to improve it or to find the exact solution. If the parabolic collocation function

$$\bar{v}_0(z) = -d_1\delta\,[1-(z/b)^2] \quad (39)$$

is used for $v_0(z)$ in Eq. 37, and the improved approximation is obtained by integrating and imposing the symmetric simple beam boundary conditions on $v_0(z)$, then the error between the two estimates $\bar{v}_0(z)$ and $\tilde{v}_0(z)$ is minimized to give d_1,

$$d_1 = \frac{1}{A\sum_{i=0}^{\infty}\frac{F_i}{[1+\Gamma]^{2i}} + \frac{255}{248}} \quad \text{.......... (40)}$$

Where $A=sb^3/(2ßEI)$, $\Gamma=t/b$, and $\delta=5sb^4p/(24EI)$. In deriving Eq. 40 from Eq. 38, the cot function was replaced by its power series expansion. F_i are dimensionless coefficients derived from those of that expansion. Values of the first 15 terms are shown in Table 2. Then

$$\sigma_y(z=0) = p\frac{5Ad_1}{24[1+\Gamma]}\int_{-1}^{1} u\cot\frac{\pi u}{2[1+\Gamma]}\ du - p \quad \text{.......... (41)}$$

$$R_v = \frac{V_{\max}}{-pb} = \frac{EIv_0'''(b)}{-spb} = \frac{5Ad_1}{48[1+\Gamma]}\int_{-1}^{1}(1-u^2)\cot\frac{\pi[1+u]}{2[1+\Gamma]}\ du + 1 \quad \text{.......... (42)}$$

$$R_m = \frac{EIv_0''(0)}{0.5spb^2} = \frac{M_{\max}}{0.5pb^2} = \frac{5Ad_1}{12\pi}\int_{-1}^{1}(1-u^2)\ln\left|\frac{\sin\frac{\pi[1+u]}{2[1+\Gamma]}}{\sin\frac{\pi u}{2[1+\Gamma]}}\right|\ du + 1 \quad \text{.......... (43)}$$

These values depend on both A (the relative stiffness of soil and lagging) and Γ (=t/b, the ratio of soldier pile flange width to lagging span). They can be expressed as

$$R_v = \frac{V_{\max}}{-pb} = -\frac{SA}{KA + \frac{255}{248}} + 1 \quad (44)$$

$$R_m = \frac{M_{\max}}{0.5pb^2} = -\frac{MA}{KA + \frac{255}{248}} + 1 \quad (45)$$

Where the coefficients *K*, *S*, and *M*, which depend only on Γ alone, are given in Table 3. When Γ becomes large, it represents wide piles and short-span lagging, and *K*, *S*, and *M* are seen to approach the values used in Eqs. 22 and 23, as they should. The maximum value *A* for which the solution is valid is the one which gives a zero pressure against the lagging at mid span. It is found by setting the right hand side of Eq. 41 to zero

$$A_{\max} = \frac{255}{248}\left[\sum_{i=0}^{\infty} A_i [1+\Gamma]^{2i}\right]^{-1} \quad (46)$$

Where A_i are dimensionless coefficients, the first 15 values of which are calculated and shown in Table 2. The value of $A_{\max}$ for different values of Γ can be found in Table 3.

The exact solution to Eq. 36 can be found by methods similar to those used for the single bay problem. It is simplest to do it for a specific value of Γ. For Γ=0, the domain of *z* in Eq. 25 is the same as the domain of *z* in the deflection found by integrating Eq. 34 with respect to *z*. Thus the exact solution for Γ=0 can be expressed as a Fourier series. The results are

$$\frac{\sigma(z)}{p} = -2A\sum_{n=1}^{\infty}(-1)^n \frac{1+\frac{(\pi n)^2 C_5}{pb^2}}{(\pi n)^3 + A}\cos\frac{\pi nz}{b} - 1 \quad (47)$$

Table 2

Coefficients for infinite lagging		
i	F_i	A_i
0	-0.2030123	0.0622459
1	0.0727221	0
2	0.0139759	0.0067985
3	0.0055064	0.0043017
4	0.0027687	0.0025375
5	0.0015905	0.0015433
6	0.0009971	0.0009872
7	0.0006657	0.0006635
8	0.0004662	0.0004657
9	0.0003390	0.0003389
10	0.0002541	0.0002541
11	0.0001954	0.0001954
12	0.0001534	0.0001534
13	0.0001226	0.0001226
14	0.0000996	0.0000996
15	0.0000819	0.0000819

Table 3

Modification Factors for Moment and Shear Coefficients				
Γ	A_{max}	K	S	M
100	16.52	0.2030052	0.1326220	0.2103711
10	16.52	0.2024103	0.1320268	0.2097763
1	16.39	0.1838596	0.1130738	0.1912869
.55	16.11	0.1698144	0.0980986	0.1773764
.5	16.04	0.1673006	0.0953465	0.1748962
.45	15.96	0.1644723	0.0922199	0.1721091
.4	15.86	0.1612703	0.0886387	0.1689586
.35	15.73	0.1576189	0.0844972	0.1653727
.3	15.58	0.1534204	0.0796510	0.1612586
.25	15.38	0.1485441	0.0738954	0.1564934
.2	15.12	0.1428104	0.0669248	0.1509093
.15	14.77	0.1359604	0.0582474	0.1442670
.1	14.31	0.1275980	0.0469715	0.1362017
0	12.73	0.1030738	0.0000002	0.1124564

$$\frac{V(z)}{pb} = -2A\sum_{n=1}^{\infty}(-1)^n \frac{1+\dfrac{(\pi n)^2 C_5}{pb^2}}{\pi n[(\pi n)^3 + A]}\sin\frac{\pi n z}{b} - \frac{z}{b} \quad \text{(48)}$$

$$\frac{M(z)}{0.5pb^2} = -4\sum_{n=1}^{\infty}(-1)^n \frac{\pi n}{(\pi n)^3 + A}\cos\frac{\pi nz}{b} + 4A\sum_{n=1}^{\infty}(-1)^n \frac{\frac{C_5}{pb^2}}{(\pi n)^3 + A}\cos\frac{\pi nz}{b} + \frac{2C_5}{pb^2} \quad \text{......................} (49)$$

At $z = b$, $M(z)=0$ and $C_5/(pb^2)$ can be found as

$$\frac{C_5}{pb^2} = \frac{2\sum_{n=1}^{\infty}\frac{\pi n}{(\pi n)^3 + A}}{1 + 2A\sum_{n=1}^{\infty}\frac{1}{(\pi n)^3 + A}} \quad \text{......} (50)$$

A_{max} in the exact solution (Eq. 47) gives A_{max}=11.53, compared to 12.73 with the approximation method at Γ=0. The error in A_{max} is thus 10% but that in R_v and R_m is less than 2% . Also, from the exact solution for a single bay lagging, or for large Γ and multiple bays, the error was less than 1%. Thus when using Table 3 to obtain the modification factors the approximate and exact solutions should be expected to differ by 1% to 2%. Plots of R_v and R_m are shown in Figs. 6 and 7, in which the curves end at $0.91 \cdot A_{max}$, the point where the solution ceases to be valid including 10% reduction to account for the error discussed above.

Effect of including friction:

Finn [3] shows that the presence of friction between soil and wall requires a minor change in the stress function, due to $\varepsilon_z = 0$, which leads to

$$\sigma_y = \int_0^{\infty} - D\left[\frac{2\beta}{\beta+\rho} + \alpha y\right] e^{-\alpha y} \cos \alpha z \, d\alpha \quad \text{(51)}$$

Solving for D shows that the solution has the same form as in the frictionless case but $1/(2ß)$ is replaced by $2ß/[(3ß - \rho)(ß + \rho)]$. Thus Figs. 3 4 6 and 7 may be used, provided that A is calculated as

$$A = \frac{2\beta s b^3}{(3\beta - \rho)(\beta + \rho)EI} \quad \text{(52)}$$

The conditions here are slightly different from those addressed by Finn [3] since ε_z is not quite zero. Thus Eq. 52 is not strictly valid, however it acts as an upper bound on A, and so is useful.

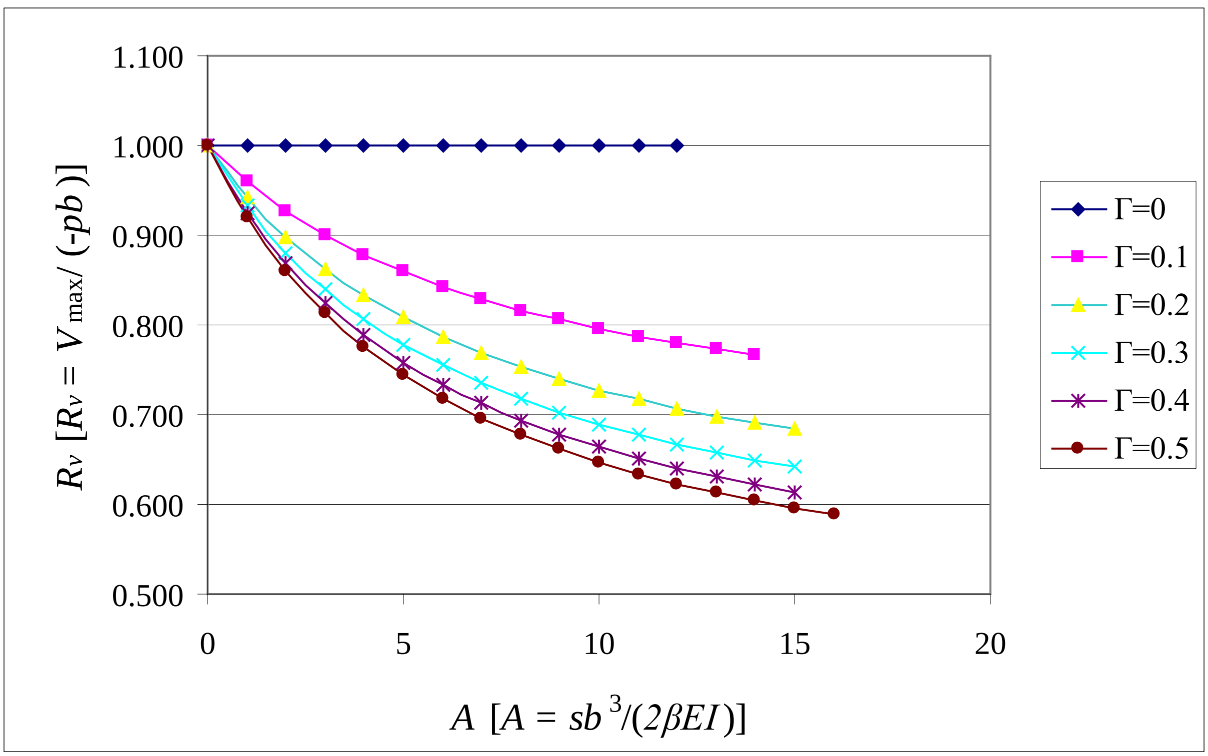

FIG.6 Dimensionless Plot of Modification Factor R_v – Infinite Bay Lagging

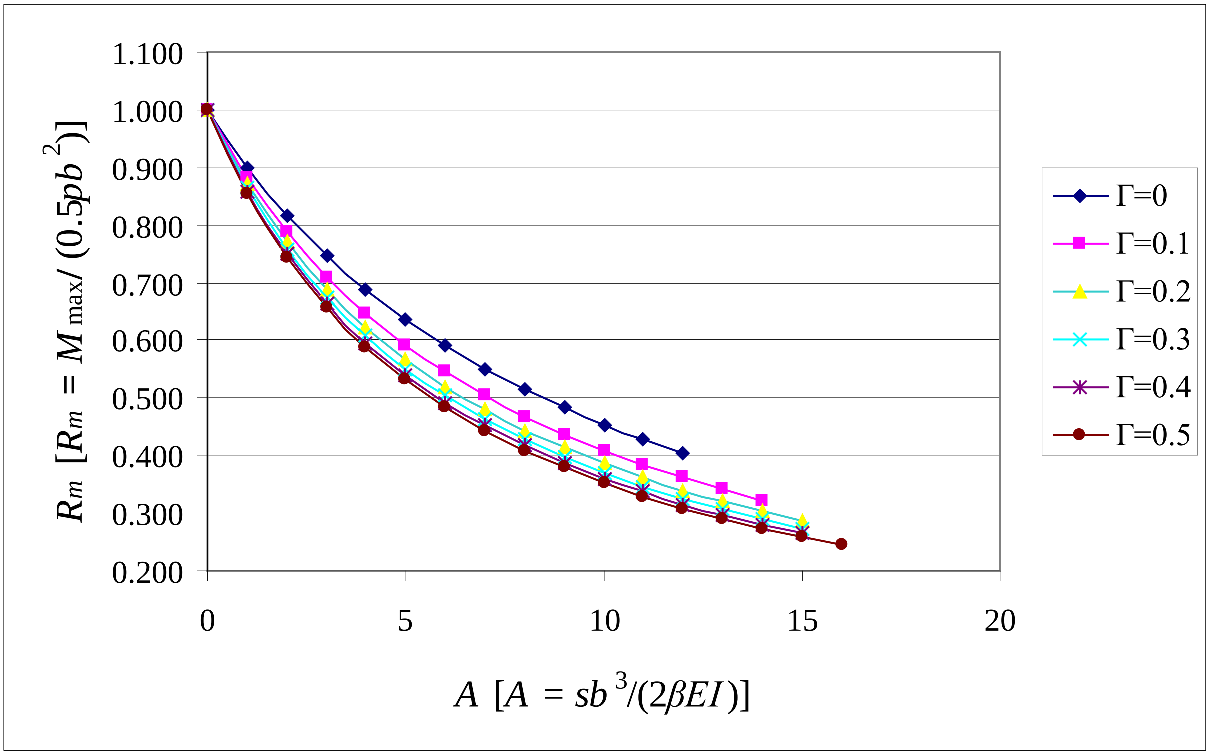

FIG.7 Dimensionless Plot of Modification Factor R_m – Infinite Bay Lagging

Examples:

Note: In the two examples which follow, p is taken as $k_0\,\gamma\,x$, where $k_0 = \mu/(1\text{-}\mu)$ and γ = unit weight of the soil, i.e. a triangular distribution of pressure. This is improbable in practice because when the lagging is installed at the bottom of the cut, the pressure behind it is zero, not $k_0\,\gamma\,x$. However, time-dependent movement of the soil will occur, increasing the pressure above this initially zero value. The triangular vertical distribution represents an upper bound for a non-yielding wall, and is used here for the sake of example.

Example 1: A temporary shoring with soldier piles that are 8'-0" o.c. and pile flange = 8.73". Wall height is 15 ft and sand is behind the wall with k_0=0.5, γ =120pcf, μ=0.3, $E_{s,\text{eff}}$=1111psi. Lagging is 3x12 Full Sawn, Douglas Fir #2 E=1800ksi, F_b=1250psi. These allowable stresses to be increased by 15% for short duration (two month) loading. Ignoring friction between lagging and soil,

s=12", b=43.63", t=4.37", Γ=t/b=0.1, I=27 in^4.

$1/ß=E_s/(1-\mu^2)$=1221 psi.

$$A = \frac{sb^3}{2\beta EI} = \frac{1221(12)(43.63)^3}{2(1{,}800{,}000)(27)} = 12.53$$

From Figs. 6 and 7: R_v=0.78 and R_m=0.35

p=0.5(120)(15)/1000=0.9 ksf

V_{max}=0.78(0.9)(1)(3.64)=2.56 k, M_{max}=0.35(0.9)(1)(3.64)^2/2=2.08 k-ft

M/S_x=2.08(12)/18=1.38 ksi < 1.25(1.15)=1.44

$1.5V_{max}/A_l$=1.5(2.56)/36=0.107 < 0.095(1.15)=0.109

Example 2: As Example 1, but including friction behind the wall

$1/\rho = E_s/[\mu(1+\mu)]$ = 2849 psi. From Eq. 52

$$A = \frac{2s\left[\frac{1}{\rho}\right]^2\left[\frac{1}{\beta}\right]b^3}{\left[\frac{3}{\rho}-\frac{1}{\beta}\right]\left[\frac{1}{\rho}+\frac{1}{\beta}\right]EI} \quad \text{.......} \quad (53)$$

$$= \frac{2(12)(2849)(2849)(1221)(43.63)^3}{[3(2849)-1221][2849+1221](1{,}800{,}000)(27)} = 13.63$$

From Figs. 6 and 7, A is in the region where tension in the soil will occur. Since this value of A is considered as an upper bound, A_{max} is used. In general if A_{max} is used for values of A larger than A_{max}, it will give conservative modification values. Thus R_v=0.77 and R_m=0.34 .

Empirical Method:

If $R_v = R_m = 0.5$ in the forgoing examples, the 3"x12" lagging would have proved easily adequate in shear, but too weak in flexure.

Discussion of Results for Lagging Walls:

Several points arise. First the beneficial effects of horizontal soil arching between piles have been shown mathematically to exist. Field evidence supports this view, but has been able to provide only empirical estimates of the extent of soil arching.

Second, the modification factors for shear and bending, R_v and R_m, are not equal. R_v is the larger, meaning that lagging is more likely to be shear critical than if R_v and R_m are assumed equal. This is particularly true if the lagging is not new, because the ends may be damaged but the mid-span is less likely to be. However, in many cases flexure will still control and then the reduction developed here will result in thinner lagging than would be allowed by the empirical value of 0.50.

The calculations here were performed using linear elastic theory. The average horizontal pressure, p, was assumed to be known a priori. It will depend on the way the wall is constructed, but does not influence the arching of the lagging between piles. Computation of p would have to take into account the details of the construction sequence being followed for a particular job. Research into this question is needed.

Extend of the Solution to Other Problems:

Because the solution is derived from elasticity other type of lagging such as concrete or steel lagging is applicable and the above charts can give a good representation of arching. For other elastic materials besides soils the solution is also given. Two such examples are a sheet of ice behind stop logs and suppose it is bricks or masonry instead of soils, channels instead of lagging and columns instead of piles, where the lagging is a channel lintel. Then the arching factors can be achieved provided the parameters for plain stress are utilized instead of plain strain.

Conclusions:

The distribution of horizontal soil pressure behind non-prismatic walls, such as those made from soldier-piles and lagging, was investigated. Both approximate and exact equations were developed for the cases of a single-bay and multiple-bays walls. The results are expressed in terms of modification factors R_v and R_m by which to multiply shears and moments in the lagging based on uniform soil pressures behind the wall.

The main conclusions are:

1. Soil arching behind pile-and-lagging walls can contribute significantly to the carriage of soil loads between the piles.

2. The extent of the arching is conveniently expressed by modification factors R_v and R_m to be applied to basic shears and moments in the lagging, calculated on the basis of soil pressure which is uniformly distributed in the horizontal direction.

3. The approximate method of calculation is computationally simpler than the exact and is quite accurate enough for practical purposes.

4. R_m is smaller than R_v, so care should be taken to check lagging for shear as well as bending stresses.

5. The R_v and R_m values presented here are likely to permit smaller lagging than would the empirical values in common use today.

6. Research is needed into the way in which the average horizontal soil pressure depends at any depth on the wall construction sequences.

Appendix 1.-References

1. M. S. Aggour and C. B. Brown, "Analytical Determination of Earth Pressure Due to Compaction", Proceedings of the Third International Conference on Numerical Methods in Geomechanics/ AACHEN/ 2-6 April 1979, pp. 1167-1174.

2. Armento, William, "Design and Construction of Deep Retained Excavations, "ASCE/SEAONC, Continuing Education Seminars, November, 1970.

3. W. D. Liam Finn, "Boundary Value Problems of Soil Mechanics", ASCE SM & FE #5 Journal of the Soil Mechanics and Foundations Division, September, 1963, p. 3648

4. Richard L. Handy "The Arch In Soil Arching" ASCE Journal of Geotechnical Engineering, March 1985, p302.

5. La Croix, Y. and Jackson, W., "Design and Construction of Support Temporary Excavations in Urban Environment", 3rd

Ohio Soil Seminar, October, 1972.

6. U. S. Department of Commerce, National Technical Information Service, PB-257 212, "Lateral Support Systems and Underpinning Vol II & III: Construction Methods" D. T. Goldberg, et al. Goldberg-Zoino & Associate, Inc., Newton Upper Falls, Mass., April, 1976, p. 29, Sect. 2.32.2, Vol. III and p. 49, Vol. II.

7. White, E. E., "Underpinning", Foundation Engineering, ed G. A. Leonards, McGraw-Hill, pp. 826-893, 1962.

Notation:

$A = \dfrac{sb^3}{2\beta EI}$;

A_i = dimensionless coefficients;

A_l = Area of lagging board;

A_{max} = value of A when σ_y at y=0 and z=0 is zero;

a_n = Fourier Series coefficients;

$B = \pi/2A$;

b = half of lagging span;

C_0 to C_5, $\overline{C}_0$ and $\overline{C}_1$ = integration constants;

D and D_n = an arbitrary constant for Φ;

d_0, $\overline{d}_0$ and d_1 = non dimensional constants used with an assumed displacement function;

E = Young's modulus for lagging;

E_s = Young's modulus for soil;

F_i = dimensionless coefficients;

I = moment of inertia of lagging cross section;

i = integer counter;

j = integer counter;

K = dimensionless coefficient;

k = integer counter;

$k_0 = \mu/(1-\mu)$ the at rest coefficient of earth pressure;

ln = natural logarithm;

M = dimensionless coefficient;

M_{max} = max moment at z=0;

n = integer counter;

p = average stress on lagging;

R_m = modification factor for moment;

R_v = modification factor for shear;

S = dimensionless coefficient;

S_x = section modulus of lagging;

s = width of lagging board in the x-direction.

t = half-width of rigid base, or half of pile flange;

u = dummy variable used in integration;

$V(\eta)$ = shear strength function;

V_{max} = max shear at $z=b$;

v = displacement function in the y-direction;

$v_0 = v$ at y=0;

$\bar{v}_0$ = a function which approximats v_0;

$\tilde{v}_0$ = an improved function for approximating v_0;

$w_0(\eta)$ = a function of _ used for simplification;

x, y and z = axes of reference;

α = dummy variable used in integration;

α_i = coefficients of the power series representation of the displacement;

$\alpha_n = n\pi/(b+t)$;

ß = $(1-\mu^2)/E_s$ for plane strain and $1/E_s$ for plane stress.

$\Gamma = t/b$;

γ = unit weight of soil;

$\delta = 5pb^4s/24EI$;

$\eta = z/b$;

λ = dummy variable used in integration;

μ = Poisson's ratio;

$\rho = \mu(1+\mu)/E_s$ for plane strain or μ/E_s for plane stress; and

σ = normal stress;

τ = shear stress;

Φ = stress function;

φ = a symbol indicating that the term a_n at n=0 is replaced by $a_0/2$;